Synthesis and Spectroscopic and Thermal Decomposition Studies of Alkali Metal Salts of 2-Oximidopropionate

Allen W. Apblett,* Galina D. Georgieva, and Joel T. Mague

Department of Chemistry, Tulane University, New Orleans, Louisiana, 70118-5698

Received September 11, 1996[⊗]

Alkali metal and tetrabutylammonium salts of 2-oximidopropionic acid were prepared by the reaction of the free acid with the respective hydroxides or carbonates in water at room temperature. These compounds were characterized by infrared and multinuclear NMR spectroscopy and thermal gravimetric analysis. The thermal decomposition of the salts occurs in the range 96−131 °C and exhibit a trend toward lower temperature with increasing size of the cation. The molecular structure of the sodium 2-oximidopropionate hydrate was determined by single-crystal X-ray crystallography. Crystal data: $C_3H_6NO_4Na$, $M = 143.08$, monoclinic, space group $P2_1/c$, $a = 13.699(2)$ Å, $b = 6.1577(7)$ Å, $c = 6.633(1)$ Å, $\beta = 103.09(2)°$, $V = 545.0(3)$ Å^3, $Z = 4$, $D_{calc} = 1.74$ g cm^{-3}, $R = 0.04$, and $R_w = 0.05$.

Introduction

Salts of 2-oximidopropionate or pyruvic acid oxime (PAO) are promising candidates for use as low-temperature precursors for metal oxide ceramics.[1,2] Typically, such salts are prepared via ligand exchange reactions of a metal chloride or nitrate with sodium pyruvic acid oxime (NaPAO). The latter compound is readily prepared by treatment of sodium pyruvate with hydroxylamine in water. Slow evaporation of the solvent typically yields enormous pincushion-like clusters of rectangular needles. These crystals cleave in layers in a similar fashion to mica suggesting a layered structure and prompting the X-ray structure reported herein.

Very few structural studies of metal PAO complexes have been reported. Previous reports have described the complexation of Cu(II), Ni(II), Co(II), Mn(II), Cr(III), Co(III), and Zn(II) with PAO.[3,4] However, the only crystal structures reported were for the complexes [BH][M(HL)L] (M = Cu, B = pyridine; M = Co, B = imidazole), where HL is the PAO anion while L is the dianion of PAO in which both the carboxylate and the oxime are deprotonated.[5,6] As well, the crystal lattice parameters of Na(PAO) were determined in an ESR investigation of γ-irradiated single crystals of the sodium and potassium salts of pyruvic acid oxime.[7]

The thermal instability of 2-oximido carboxylate complexes has been remarked upon in previous studies, and they have been used for quantitative determination of Cu(II) ions via their precipitation from solution and subsequent pyrolysis to CuO. Similar reactions have also been used to prepare metal oxide ceramics[1,2] and catalysts.[8] As well, the thermal decomposition of 2-oximido carboxylic acids is a useful synthetic route for the preparation of functionalized nitriles[9] (Scheme 1).

Scheme 1. Generation of Nitriles from 2-Oximido Carboxylic Acids

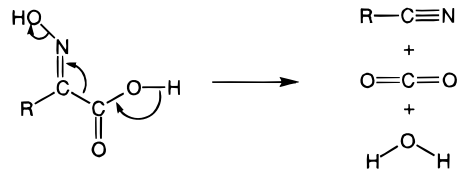

In this investigation, the thermal behavior of the alkali metal salts of pyruvic acid oxime has been investigated. Our interest in the thermochemistry of these compounds was sparked by the observation that K(PAO) was less thermally-stable than Na(PAO) when it was expected that the opposite would be true. The results of this study as well as the spectroscopic characterization of the complexes are reported herein.

Experimental Section

Sodium pyruvate, hydroxylamine hydrochloride, LiOH·H_2O, [^{n}Bu$_4$N]OH (40 wt % solution in water), Na_2CO_3, K_2CO_3, Rb_2CO_3, and Cs_2CO_3 were commercial reagents and were used without further purification. Infrared spectra were obtained as KBr pellets on a Mattson Cygnus 100 FT-IR spectrometer. ^{1}H and ^{13}C{^{1}H} NMR spectra were recorded on either a GE 400 NMR spectrometer or Bruker AC 200 spectrometer and were referenced to TMS. ^{23}Na and ^{14}N NMR spectra were recorded on a Bruker AC 200 FT NMR, and chemical shifts are reported versus 10 M NaCl and neat nitromethane, respectively. Solid-state ^{13}C CPMAS and ^{23}Na NMR spectra were recorded on Bruker DSX 300 spectrometer and referenced to TMS and NaCl, respectively. UV−visible spectra were obtained using aqueous solutions and a Hewlett Packard 8451A diode array spectrometer. Thermogravimetric studies were performed using 20−30 mg samples in a Seiko TG/DTA 220 instrument under a 100 mL/min flow of dry air. The temperature was ramped from 25 to 625 °C at a rate of 2 °C/min while the off-gases were analysed on a Fisons Thermolab mass spectrometer. The decomposition temperatures were determined from the differential thermal analysis trace using a subprogram of the Seiko TGA/DTA software that extrapolated the onset temperatures. The degree of hydration of the metal salts was determined from the observed

[⊗] Abstract published in *Advance ACS Abstracts,* May 15, 1997.

(1) Apblett, A. W.; Lei, J.; Georgieva, G. D. In *Better Ceramics Through Chemistry V*; *Mater. Res. Soc. Symp. Proc., Vol. 271*; Hampden-Smith, M. J., Klemperer, W. G., Brinker, C. J., Eds.; Materials Research Society: Pittsburgh, PA, 1992; pp 77−82.
(2) Apblett, A. W.; Georgieva, G. D. *Phosphorus Sulfur, Silicon, Rel. Elem.* **1994**, *93*−*94*, 479.
(3) Slopenko, V. V.; Lampeka, R. D.; Sliva, T. Y.; Sakhov, D. I. *Ukr. Khim. Zh.* **1990**, *56*, 675.
(4) Lampeka, R. D.; Slopenko, V. V.; Sliva, T. Y.; Khennig, K. *Ukr. Khim. Zh.* **1988**, *54*, 675.
(5) Simonov, Y. A.; Sliva, T. Y.; Mazus, M. D.; Dvorkin, A. A.; Lampeka, R. D. *Russ. J. Inorg. Chem.* **1989**, *34*, 489.
(6) Dvorkin, A. A. ; Simonov, Y. A.; Sliva, T. Y.; Lampeka, R. D.; Mazus, M. D.; Skopenko, V. V. *Russ. J. Inorg. Chem.* **1989**, *34*, 489.
(7) Hayashi, H.; Itoh, K.; Nagakura, S. *Bull. Chem. Soc. Jpn.* **1967**, *40*, 284.
(8) Apblett, A. W.; Georgieva, G. D.; Mague, J. T., Reinhardt, L. E. *Ceram. Trans.*, in press.
(9) Ahmad, A.; Spenser, I. D. *Can. J. Chem.* **1961**, *39*, 1340.

S0020-1669(96)01120-2 CCC: $14.00

dehydration step in the TGA trace (in the case of the Rb and Cs salts this was done via isothermal experiments at 90 °C). The number of waters of hydration are reproducible for samples dried in a dry air stream, but the salts are somewhat hygroscopic. Bulk pyrolyses at various temperatures were performed in ambient air in a temperature-programmable muffle furnace using ca. 2 g samples, a temperature ramp of 5 °C/min, and a hold time of 12 h. X-ray powder diffraction patterns were obtained on a Scintag XDS 2000 diffractometer using copper Kα radiation. Microanalysis for C, H, and N content was performed by Oneida Research Services or Tulane's Coordinated Instrument Facility.

Preparation of $CH_3C(=NOH)COOH$ (HPAO). The compound pyruvic acid oxime was prepared by a modification of a published procedure.[9] An aqueous solution of Na(PAO) was acidified with 2 M hydrochloric acid to a final pH of 2. The resulting solution was allowed to evaporate to dryness. The pyruvic acid oxime was extracted from the solid with warm absolute ethanol. Cooling of this solution yielded large colorless crystals of HPAO. ^{1}H NMR (DMSO-d_6): δ (ppm) 1.88 (s, 3H, CH_3), 12.28 (br s, 2H, NOH and COOH). ^{13}C{^{1}H} NMR (DMSO-d_6): δ (ppm) 10.7 (CH_3) , 148.9 (C=N), 166.0 (COO). IR (cm^{-1}) (KBr): 3224 (s, br), 3076 (s, br), 2921 (s, sh), 2697 (s, sh), 2562 (s), 1767 (m, sh), 1696 (s), 1652 (s), 1472 (s), 1420 (s), 1299 (s), 1177 (s), 1048 (s), 990 (s, sh), 907 (s), 818 (s), 766 (m), 702 (s), 535 (m), 458 (m).

Preparation of [^{n}Bu$_4$N](PAO). A 1.04 g (10 mmol) amount of HPAO in 10 mL of 95% EtOH was added to 6.50 g of a 40% solution of [^{n}Bu$_4$N]OH. Large, colorless crystals were formed upon slow evaporation of the solvent. These were isolated and air-dried to yield 1.62 g (47%), decomp pt 76.6 °C. ^{1}H NMR (D_2O): δ (ppm) 0.76 (t, ^3J(HH) = 7.6 Hz, 12H, CH_3CH$_2$CH$_2$), 1.17 (sextet, ^3J(HH) = 7.6 Hz, 8H, CH$_3$CH_2CH$_2$), 1.45 (quint, ^3J(HH) = 7.6 Hz, 8H, CH$_3$CH$_2$CH_2), 1.82 (s, 3H, CH_3, PAO), 2.99 (t, ^3J(HH) = 8.80 Hz, 8H, NCH$_2$). ^{13}C-{^{1}H} NMR (D_2O): δ (ppm) 11.9 (CH_3, PAO), 13.7 (CH_3CH$_2$), 20.0 (CH$_3$CH_2), 24.0 (CH$_3$CH$_2$CH_2), 59.0 (NCH$_2$) 156.1 (C=N), 171.5 (COO). IR (cm^{-1}) (KBr): 3453 (s), 3189 (s), 3057 (s), 2966 (s), 2877 (s), 1734 (s, sh), 1653 (s), 1631 (sh), 1490 (s), 1469 (s), 1458 (s), 1381 (s), 1364 (s), 1196 (m), 1180 (m, sh), 1152 (m), 1018 (s), 958 (m), 886 (s), 836 (w), 738 (m), 706 (s), 648 (w), 631 (w), 587 (w), 526 (w).

Preparation of Li(PAO)·1.4H_2O. LiOH·H_2O (0.42 g, 10.0 mmol) and HPAO (1.03 g, 10.0 mmol) were combined in 25 mL of water. The solvent was removed by rotary evaporation to give a white solid, which was washed with acetone and air dried to yield 1.24 g (97%) of Li(PAO)·1.4H_2O, decomp pt 131 °C. Anal. Calcd for $LiC_3H_4O_3N$·1.4H_2O: C, 26.87; H, 5.11; N, 10.43. Found: C, 26.87; H, 4.94; N, 10.12. ^{1}H NMR (DMSO-d_6): δ (ppm) 1.83 (3H, CH_3), 12.03 (br s, ^{1}H, NOH). ^{13}C{^{1}H} NMR (DMSO-d_6): δ (ppm) 11.8 (CH_3), 154.9 (C = N), 168.7 (COO). IR (cm^{-1}) (KBr): 3544 (s, sh), 3461 (s, sh), 3415 (s), 3255 (m, sh), 1660 (m, sh), 1637 (s), 1619 (s), 1459 (w), 1384 (m), 1363 (w), 1215 (w), 1018 (w), 965 (w), 911 (w), 848 (w), 785 (w), 733 (m), 645 (m).

Preparation of Na(PAO)·H_2O. Na_2CO_3 (10.6 g, 100.0 mmol) was slowly added to a solution of sodium pyruvate (22.0 g, 200.0 mmol) and hydroxylamine hydrochloride (13.9 g, 200.0 mmol) in 150 mL of water. The reaction mixture deposits Na(PAO)·H_2O as colorless crystals after standing at 5 °C for several days. These crystals were filtered off, washed with water, and air dried to provide a yield of 24.2 g (83%), decomp pt 121.6 °C. ^{1}H NMR (DMSO-d_6): δ (ppm) 1.84 (s, 3H, CH_3), 12.12 (br s, ^{1}H, NOH). ^{13}C{^{1}H} NMR (D_2O): δ (ppm) 11.8 (CH_3), 156.4 (C=N), 171.3 (COO). Solid-state ^{13}C CPMAS NMR: δ (ppm) 12.2 (CH_3), 153.5 (C=N), 171.7 (COO). ^{14}N NMR (D_2O): δ −26.3 ppm. ^{23}Na NMR (D_2O): δ −0.89 ppm. Solid-state ^{23}Na{^{1}H} NMR: δ: −9.86 ppm. IR (cm^{-1}) (KBr): 3258 (s, br), 2931 (m, sh), 1661 (s), 1599 (s), 1572 (s), 1456 (s), 1375 (s), 1359 (s), 1213 (m), 1363 (w), 1213 (s), 1008 (s), 966 (s), 852 (s), 793 (s), 727 (s), 702 (s, sh), 597 (s), 542 (m), 457 (w). UV−visible H_2O: 197 nm.

Preparation of K(PAO)·H_2O. K_2CO_3 (2.76 g, 20.0 mmol) and HPAO (4.12 g, 40.0 mmol) were combined in 50 mL water. After evolution of carbon dioxide had ceased, the solvent was removed by rotary evaporation to give a white solid, which was washed with acetone and air dried to yield 5.12 g (80%) of K(PAO)·H_2O, decomp pt 108.3 °C. ^{1}H NMR (DMSO-d_6): δ (ppm) 1.77 (s, 3H, CH_3), 11.24 (br s, 1H, NOH). ^{13}C{^{1}H} NMR (D_2O): δ (ppm) 11.7 (CH_3), 156.4 (C=N), 171.4 (COO). IR (cm^{-1}) (KBr): 3487 (s, sh), 3416 (s), 3211 (s, sh), 1662 (m), 1599 (s), 1570 (s), 1463 (s), 1373 (s), 1360 (s), 1212 (m), 1108 (w), 1009 (s), 967 (m), 852 (m), 791 (m), 725 (m), 604 (w), 475 (m).

Table 1. Crystallographic Data for $NaC_3H_4NO_3$·H_2O

formula	$C_3H_6NO_4Na$	2θ range, deg	1.0−54.0
fw	143.08	scan type	ω−2θ
cryst syst	monoclinic	scan width, deg	0.90 + 0.20 (tan θ)
space group	$P2_1/c$ (No. 14)		
a, Å	13.699(2)	scan, speed, deg·min^{-1}	1.26−16.4
b, Å	6.1577(7)	no. data collcd	1358
c, Å	6.633(1)	no. unique data	1189
b, deg	103.09(2)	conditon for obs data	$I > 3\sigma(I)$
V, Å^3	545.0(3)	no. obs data	916
Z	4	no. variables	106
d_{calc}, g·cm^{-3}	1.74	R^a	0.04
μ, cm^{-1}	2.11	$R_w{}^b$	0.05
range trans factors	0.821−0.998	GOF^c	1.73

^{a} $R = \sum||F_o| - |F_c||/\sum|F_o|$. ^{b} $R_w = [\sum(w||F_o| - |F_c||)^2/\sum|F_o|^2]^{1/2}$, where $w = I/\sigma^2(F_o)$ with $\sigma(F_o) = \sigma(F^2)/2F$ and $\sigma(F^2) = [\sigma^2(I) + (0.4F^2)^2]^{1/2}$. ^{c} GOF = $[\sum(w||F_o| - |F_c||)^2/\sum(N_o - N_v)]^{1/2}$, where N_o and N_v are, respectively, the number of observations and variables.

Preparation of Rb(PAO)·H_2O. Rb_2CO_3 (1.15g, 5.00 mmol) and HPAO (1.03g, 10.0 mmol) were combined in 25 mL of water. After evolution of carbon dioxide had ceased, the solvent was removed by rotary evaporation and the resulting white solid was washed with acetone and air dried to yield 1.95 g (95%) of Rb(PAO)·H_2O, decomp pt 103 °C. ^{1}H NMR (DMSO-d_6): δ (ppm) 1.77 (s, 3H, CH_3), 12.09 (br s, 1H, NOH). ^{13}C{^{1}H} NMR (DMSO-d_6): δ (ppm) 11.3 (CH_3), 156.2 (C=N), 171.2 (COO). IR (cm^{-1}) (KBr): 3550 (s), 3467 (s, sh), 3409 (s), 3243 (m, sh), 1638 (s), 1625 (s), 1459 (w), 1388 (w), 1144 (w), 1112 (w), 840 (w), 618 (s).

Preparation of Cs(PAO)·0.71H_2O. HPAO (1.03 g, 10.0 mmol) was added to a solution of Cs_2CO_3 (1.63 g, 5.00 mmol) in 25 mL of water. After the evolution of carbon dioxide had stopped, the solvent was removed by rotary evaporation. The resulting white solid was washed with acetone and air dried to yield 2.25 g (96%) of Cs(PAO)·H_2O, decomp pt 96.2 °C. Anal. Calcd for $CsC_3H_4O_3N$·0.71H_2O: C, 14.54; H, 2.20; N, 5.65. Found: C, 14.54; H, 2.16; N, 5.54. ^{1}H NMR (DMSO-d_6): δ (ppm) 1.75 (3H, CH_3), 10.55 (br s, ^{1}H, NOH). ^{13}C{^{1}H} NMR (D_2O): δ (ppm) 12.0 (CH_3), 156.7 (C=N), 171.7 (COO). IR (cm^{-1}) (KBr): 3557 (s), 3478 (s), 3418 (s), 3240 (m, sh), 1639 (s), 1618 (s), 1386 (s), 1204 (w), 1004 (w), 990 (w), 725 (w).

X-ray Structure Determination of Na(PAO)·H_2O. The growth of single crystals of sodium pyruvic acid oxime is a challenging task due to a propensity toward extensive twinning. This difficulty was commented on by Hayashi et al., who prepared single crystals for irradiation studies by careful evaporation of a saturated aqueous solution.[7] In the present investigation, crystals of Na(PAO)·H_2O suitable for X-ray analysis were obtained by slow evaporation of a solution in 50:50 water/acetone at 20 °C. A single crystal measuring 0.40 × 0.23 × 0.40 mm was mounted on a thin glass fiber and coated with a thin film of epoxy cement. General procedures for crystal orientation, unit cell determination, and refinement and data collection on the CAD-4 diffractometer have been published.[10] The crystallographic data for Na(PAO)·H_2O are summarized in Table 1. The monoclinic cell indicated by the CAD-4 software was confirmed by the observation of 2/m diffraction symmetry, and the space group was uniquely determined by the systematic absences observed in the final data set. The space group and cell parameters are essentially the same as that reported by Hayashi et al.[7] with the only major difference being the β angle which they report as 104.0°, 1 deg larger than in this study. The raw intensity data were corrected for Lorentz and polarization effects and for absorption based on Ψ scans of four reflections with χ near 90°. Only statistical fluctuations in the intensity monitors were observed. Equivalent reflections were averaged giving an agreement factor of 0.022 on F. The structure was solved by direct methods (SIR88),[11] which provided locations for all non-hydrogen atoms. Full-

(10) Mague, J. T.; LLoyd, C. L. *Organometallics* **1988**, *7*, 983.

matrix, least-squares refinement of this model using neutral atom scattering factors for C, O, and N and treating sodium as Na^+ followed by calculation of a difference map provided locations for all hydrogen atoms. These were successfully refined using isotropic thermal parameters. The final difference map was essentially featureless.

Results and Discussion

The preparation of sodium and potassium derivatives of pyruvic acid oxime (PAO) and their partial characterization have previously been reported.[7,12] In this investigation, several approaches were employed for the preparation of alkali metal PAO complexes. The pyruvic acid oxime anion is most conveniently prepared via reaction of sodium pyruvate with hydroxylamine in a fashion similar to the method of Occupanti et al.[12] This reaction was performed by generating the hydroxylamine in situ in an aqueous solution of the 2-keto acid via the interaction of hydroxylamine hydrochloride with sodium carbonate (eq 1). Slow evaporation and cooling of the aqueous solution thus obtained results in the growth of very big (up to 5 cm) colorless needle-shaped crystals which typically grow in large starburstlike clusters.

$$2CH_3C(=O)COONa + 2[H_3NOH]Cl + Na_2CO_3 \rightarrow 2CH_3C(=NOH)COONa + CO_2 + 2NaCl + 3H_2O \quad (1)$$

The preparation of other alkali metal salts of pyruvic acid oxime relies on the conversion of the sodium salt to the free acid. This is readily accomplished by treatment of Na(PAO) with dilute hydrochloric acid.[9] In this investigation, rather than using solvent extraction to separate the HPAO from the sodium chloride by-product, the HPAO was isolated by evaporating the reaction mixture to dryness and then extracting the resulting solid with warm (70 °C) absolute ethanol. This approach has the advantage that crystals of HPAO are readily obtained by cooling the resulting ethanolic solution. The product obtained in this fashion is highly pure, and any contamination with sodium or chloride is below the detection limits of X-ray fluorescence spectroscopy (ca. 10 ppm).

The lithium and tetra-*n*-butylammonium derivatives of PAO were prepared by neutralization of the parent acid with the corresponding hydroxides (eq 2). Similarly, the potassium, rubidium, and cesium derivatives were prepared via reaction of the metal carbonates with the parent acid (eq 3).

$$MOH + CH_3C(=NOH)COOH \rightarrow CH_3C(=NOH)COOM + H_2O \quad (2)$$

$$M = Li, {}^nBu_4N$$

$$M_2CO_3 + 2CH_3C(=NOH)COOH \rightarrow CH_3C(=NOH)COOM + CO_2 + H_2O \quad (3)$$

$$M = K, Rb, Cs$$

Crystal Structure of Na(PAO)·H_2O. The structure of Na(PAO)·H_2O is composed of chains of $Na^+(PAO)^-$ units (Figure 1) that are linked to each other via bridging carboxylates. The oxygen atom, O(2), which forms this bridge is also attached to a neighboring sodium atom on an adjacent chain so that layers are formed perpendicular to the *c*-axis via bridging carboxylates. Relevant bond lengths and angles are given in Tables 2 and 3, respectively. The sodium atom is heptacoordinated (Figure 2)

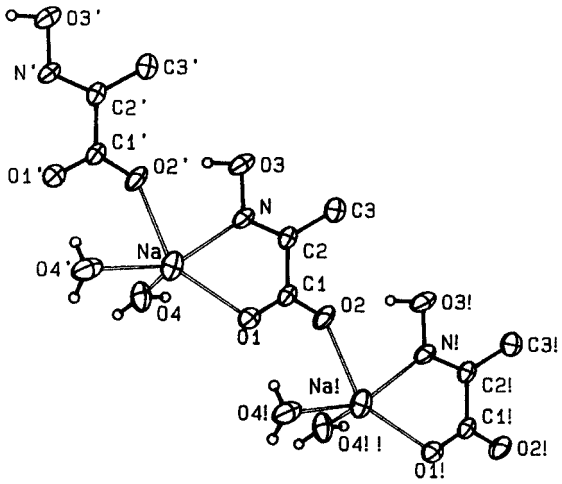

Figure 1. View of the $Na^+(PAO)^-$ chain. Thermal ellipsoids are drawn at the 70% probability level, and hydrogen atoms are arbitrarily small for clarity.

Table 2. Bond Distances (Å) for $NaC_3H_4NO_3·H_2O$

Na−O(1)	2.490(2)	N−C(2)	1.281(2)
Na−O(2)′	2.585(2)	C(1)−C(2)	1.515(2)
Na−O(2)″	2.588(2)	C(2)−C(3)	1.487(2)
Na−O(4)	2.391(2)	C(3)−H(1)	0.99(3)
Na−O(4)′	2.530(2)	C(3)−H(2)	1.00(3)
Na−O(4)″	2.917(2)	C(3)−H(3)	0.98(3)
Na−N	2.440(2)	O(3)−H(4)	0.90(4)
O(1)−C(1)	1.259(2)	O(4)−H(5)	0.86(4)
O(2)−C(1)	1.255(2)	O(4)−H(6)	0.79(3)
O(3)−N	1.396(2)		

Table 3. Interbond Angles (deg) for $NaC_3H_4NO_3·H_2O$

O(1)−Na−O(2)′	133.94(6)	O(4)′−Na−O(4)″	72.17(5)
O(1)−Na−O(2)″	91.02(5)	O(4)′−Na−N	151.68(5)
O(1)−Na−O(4)	82.37(5)	O(4)″−Na−N	131.62(5)
O(1)−Na−O(4)′	141.57(6)	O(3)−N−C(2)	114.3(1)
O(1)−Na−O(4)″	69.52(5)	O(1)−C(1)−O(2)	124.7(2)
O(1)−Na−N	64.08(5)	O(1)−C(1)−C(2)	118.2(2)
O(2)′−Na−O(2)″	101.48(5)	O(2)−C(1)−C(2)	117.1(2)
O(2)′−Na−O(4)	85.67(5)	N−C(2)−C(1)	112.2(2)
O(2)′−Na−O(4)′	85.41(5)	N−C(2)−C(3)	127.5(2)
O(2)′−Na−O(4)″	155.34(5)	C(1)−C(2)−C(3)	120.3(2)
O(2)′−Na−N	73.03(5)	C(2)−C(3)−H(1)	112(2)
O(2)″−Na−O(4)	172.53(5)	C(2)−C(3)−H(2)	113(2)
O(2)″−Na−O(4)′	81.39(5)	C(2)−C(3)−H(3)	110(2)
O(2)″−Na−O(4)″	82.90(5)	H(1)−C(3)−H(2)	109(2)
O(2)″−Na−N	84.96(5)	H(1)−C(3)−H(3)	106(2)
O(4)−Na−O(4)′	101.63(5)	H(2)−C(3)−H(3)	107(2)
O(4)−Na−O(4)″	91.48(5)	N−O(3)−H(4)	94(2)
O(4)−Na−N	95.21(6)	H(5)−O(4)−H(6)	112(3)

with two of the coordination sites occupied by the nitrogen and carboxylate oxygen donor atoms from the chelated PAO ligand. The Na−O(1) and Na−N bond distances in this metallacycle (Table 2) are 2.490(2) and 2.440(2) Å, respectively. Two other coordination sites of the sodium ion are occupied by water molecules with Na−O(4) and Na−O(4)′ bond distances being 2.391(2) and 2.530(2) Å. The fifth and sixth coordination sites in the sphere of the sodium atom are occupied by oxygen atoms from bridging carboxylate groups of adjacent Na(PAO) complexes, and the corresponding bond distances for Na−O(2)′ and Na−O(2)″ are 2.585(2) and 2.588(2) Å, respectively. The coordination sphere of the sodium atom is completed by a weak long-range coordination of another water molecule at a distance of Na−O(4)″ = 2.917(2) Å. All of the water molecules unsymmetrically cap three adjacent sodium ions.

The partial negative charge in the carboxylate moiety of the oximino carboxylate ligand is fully delocalized. This is evidenced by the practically equal O(1)−C(1) and O(2)−C(1)

(11) Burla, M. C.; Camalli, M.; Cascarino, G.; Giaconsazzo, C.; Polidori, G.; Spagana, R.; Viterno, D. *J. Appl. Crystallogr.* **1989**, *22*, 389.
(12) Occupanti, G.; Pratt, L. *J. Chem. Soc., Dalton Trans.* **1973**, 1699.

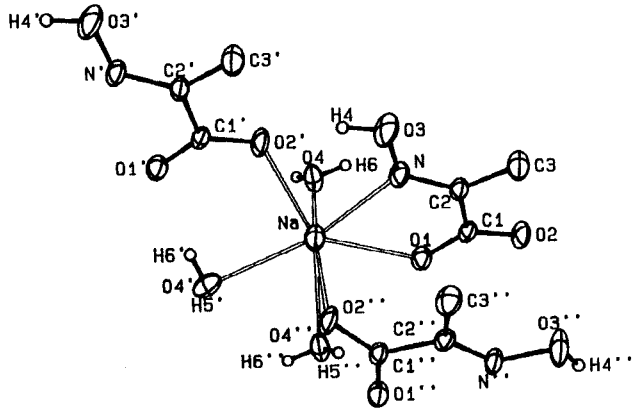

Figure 2. Perspective view of the coordination about sodium which also shows the interaction Na−O(2)″ which occurs between adjacent chains. Thermal ellipsoids are drawn at the 70% probability level, and hydrogen atoms are arbitrarily small for clarity.

Table 4. Characteristic IR Vibrational Frequencies (cm^{-1}) of PAO Salts

compd	ν(C═N)	ν_{as}(COO)	ν_s(COO)	ν(N−O)
HPAO	1652	1696	1420	1048
$^nBu_4$NPAO	1653	1631	1381	1018
LiPAO·1.4H_2O	1660	1619	1384	1018
NaPAO·H_2O	1661	1599	1375	1008
KPAO·H_2O	1662	1599	1373	1009
RbPAO·H_2O	1638	1625	1388	1085
CsPAO·0.71H_2O	1639	1618	1386	1004

bond distances (1.259(2) and 1.255(2) Å, respectively). These bond distances have intermediate values between those of the carbon−oxygen single and double bonds (1.36 and 1.23 Å, respectively[13]). The remaining bond distances in the five-membered metallocycle have values of 1.515(2) and 1.281(2) Å for C(1)−C(2) and N−C(2) and are similar to the ones reported for the related PAO complexes of Cu^{2+} (1.49(1) and 1.27(1) Å, respectively) and Ni^{2+} (1.50(2) and 1.28(1) Å, respectively).[5,6] As well, all of the atoms of the chelated ligand are essentially coplanar.

One contrast between the structure of Na(PAO) and the previously reported nickel and copper PAO complexes is the long sodium−nitrogen bond distance. This bond length is 2.440(2) Å while the Cu−N and Ni−N bond distances are 1.925(6) and 2.021(8) Å, respectively.[5,6] Although, the ionic radius for Na^+ (0.97 Å) is somewhat larger then those of Cu^{2+} (0.72 Å) and Ni^{2+}(0.69 Å) ions,[14] this dissimilarity is not sufficient to account for differences in the metal−nitrogen bond lengths.

Comparison of the structure of Na(PAO)·H_2O to that of a prototypical hydrated sodium carboxylate such as sodium acetate trihydrate[15] reveals a number of significant differences. The latter compound is also composed of chains of sodium−oxygen polyhedra that are bound into sheets by hydrogen-bonded water molecules. However, the carboxylate of the acetate ion is monodentate and has a considerably shorter contact (2.417 Å) to the sodium ion than the PAO anion.

Spectroscopic Characterization of PAO Complexes. Several characteristic infrared vibrational frequencies of the PAO salts are summarized in Table 4. The assignment of these frequencies is based on literature data for previously reported PAO complexes[3,4] which utilized ^{15}N isotopic labeling to identify these bands. A characteristic feature of the IR spectra of the PAO complexes is the significant lowering of the vibrational frequencies of the assymetric carboxylate stretch by 77−95 cm^{-1} compared to that of the parent acid. The decrease of these frequencies for the tetra-*n*-butylammonium salt of PAO (in which the cation is noncoordinating) is slightly smaller (65 cm^{-1}). Thus, the changes in the asymmetric carboxylate stretching frequency observed for the alkali metal PAO salts may be attributed to both the deprotonation and delocalization of the negative charge in the carboxylate as well its coordination to the metal centers. Such effects are typical for metal carboxylates.[16] The coordination of the nitrogen atom of the oximido moiety in the PAO complexes of the lighter alkali metals (Li, Na, K) does not significantly affect the vibrational frequency corresponding of the C═N stretch and is consistent with the data obtained in previous studies.[3,4] On the other hand, this band occurs at slightly reduced frequencies (by ca. 17 cm^{-1}) for the rubidium and cesium salts. The vibrational frequencies attributable to the N−O stretch are lowered by 30−44 cm^{-1} in the alkali metal salts of PAO from that observed for the parent acid. This trend is opposite to that observed for transition metal derivatives of PAO, in which an increase in these frequencies was observed.[3,4] This difference may be a result of the weak coordination of the nitrogen atom of the oximido group in the alkali metal salts, as indicated by the elongated Na−N bond distance in Na(PAO)·H_2O. This conclusion is supported by the observation of a highly similar frequency of the N−O stretch for PAO when its counterion is the noncoordinating tetrabutylammonium cation.

Table 5. ^1H and ^{13}C NMR Chemical Shifts of PAO Salts

	^1H NMR		^{13}C NMR		
compd	CH_3	OH[a]	CH_3	C═N	COO
HPAO	1.88	12.28	10.9	148.9	166.0
$^nBu_4$N(PAO)	1.82		11.9	156.1	171.5
Li(PAO)·1.4H_2O	1.83	12.03	11.8	154.9	168.7
Na(PAO)·H_2O	1.84	12.12	11.8	156.4	171.3
			12.2[b]	153.5[b]	171.7[b]
K(PAO)·H_2O	1.77	12.24	11.7	156.4	171.4
Rb(PAO)·H_2O	1.77	12.09	11.3	156.2	171.2
Cs(PAO)·0.71H_2O	1.75	10.55	12.0	156.7	171.7

[a] These chemical shifts were observed in dry DMSO-d_6 and are attributable to the oxime protons and those of the waters of crystallization which undergo rapid exchange. [b] Solid-state ^{13}C-CPMAS NMR.

The ^1H and ^{13}C NMR spectral data for these compounds are summarized in Table 5. The ^1H NMR spectra of the PAO anions display two resonances, one for the methyl and one for the oxime protons. Since the methyl and oxime protons are remote from the carboxylic acid moiety of the PAO ligand, no significant changes in their chemical shift are observed upon deprotonation. The chemical shift for the CH_3 group in the PAO salt is within the range of 1.77−1.87 ppm, while the protons of the oxime give rise to resonances in the range 10.55−12.79 ppm. These chemical shifts are not significantly different from the corresponding ones for the parent acid which are observed at 1.88 and 12.28 ppm, respectively. The ^{13}C NMR spectra of the PAO are more indicative of the changes in the local electron density in the ligand as a result of its deprotonation. As expected, the methyl carbon, with a chemical shift in the range 11.0−12.0 ppm, is less affected by the deproto-

(13) Mehrota, R., Bohra, R. *Metal Carboxylates*; Acad. Press: New York, 1983.
(14) *CRC Handbook of Chemistry and Physics*; 64th ed.; Weast, R. C., Ed.; CRC Press Inc.: Boca Raton, FL, 1984; F170.
(15) Wei, K. T.; Ward, D. L. *Acta Crystallogr.* **1977**, *B33*, 522.
(16) Smith, A. L. Applied Infrared Spectroscopy-Fundamentals, Techniques and Analytical Problem-Solving. In *Analysis: a Series of Monographs on Analytical Chemistry and its Applications*; Elving, P. J., Winefordner, J. D., Kolthoff, I. M., Eds.; John Wiley & Sons: New York, 1979; Vol. 54.

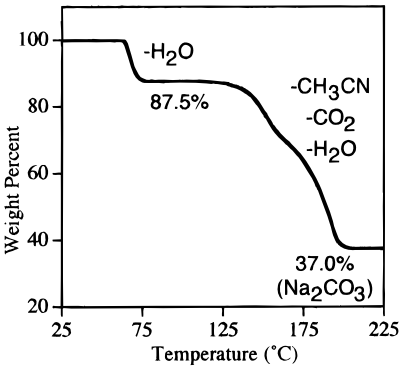

Figure 3. Thermogravimetric analysis (TGA) trace for Na(PAO)·H_2O in dry nitrogen with a heating rate of 2 °C/min.

nation and its signal is shifted only about 0.5−1.0 ppm downfield from the corresponding signal of the parent acid (10.7 ppm). The signals of the carbon atoms of the oximido and carboxylate groups undergo more significant downfield shifts from the parent acid upon removal of the proton, 6 to 7.8 ppm for C = N and 2.7 to 5.7 ppm for COO.

With the exception of the lithium PAO salt, the ^{13}C NMR chemical shifts of all the alkali metal PAO salts in D_2O fall into a very narrow range indicating that the salts of the larger alkali metals are substantially dissociated in aqueous media. This conclusion is supported by the similarity of the chemical shifts of the tetra-*n*-butylammonium salt where coordination of the anion to the cation is not possible. As well, the ^{23}Na NMR chemical shift of Na(PAO) in D_2O solution is only 0.89 ppm upfield from that of aqueous sodium chloride while, in the solid state, the ^{23}Na chemical shift is 9.86 ppm upfield relative to NaCl (the measured quadrupolar coupling constant was found to be 817.4 kHz). The ^{14}N NMR spectrum of Na(PAO) in D_2O exhibits a broad resonance at −26.3 ppm relative to neat nitromethane that has a width at half-height of 4250 Hz. This chemical shift is within the range observed for typical nonco-ordinated oximes.[17]

Thermal Behavior of Alkali Metal PAO Salts. The thermal gravimetric analysis of Na(PAO)·H_2O (Figure 3) exhibits two weight-loss steps. The lower temperature weight change with an onset of 63 °C is endothermic and corresponds to the dehydration of the sodium salt. Remarkably, the dehydration does not destroy the crystallinity of the salt and is reversible. The X-ray diffraction pattern of a bulk sample dried at 130 °C is significantly different from that of the hydrated salt, but it slowly reverts back to the original pattern upon exposure to humid air (Figure 4). The next weight loss of Na(PAO)·H_2O occurs at 122 °C and is exothermic. Simultaneous analysis of the off-gases at this temperature by mass spectroscopy indicates that decomposition of the anion is occurring to yield the expected products: water, acetonitrile, and carbon dioxide. The metal-containing residue from this decomposition has a mass which corresponds to formation of sodium carbonate. The X-ray diffraction pattern of a bulk sample of Na(PAO)·H_2O pyrolyzed at 170 °C (Figure 4) confirms this identification since it matches that reported for natrite (Na_2CO_3).

The results of the thermal analysis of the other PAO salts were similar to that of the sodium salt. Surprisingly, however, the thermal decomposition temperature of the alkali metal salts decreases with increasing ionic radii of the metal ions (Figure 5) and is, therefore, opposite to the trend observed for the alkali metal carbonates. Simple considerations based on the ionic

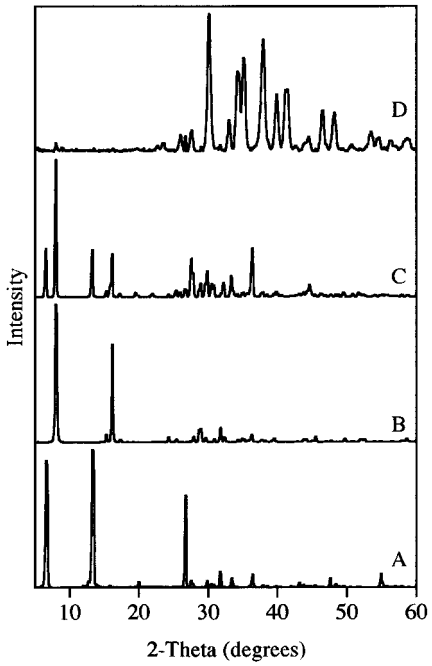

Figure 4. X-ray powder diffraction patterns for (A) Na(PAO)·H_2O, (B) Na(PAO)·H_2O dried at 130 °C for 12 h, (C) sample B exposed to humid air for 1 week, and (D) Na(PAO)·H_2O pyrolyzed at 170 °C for 4 h.

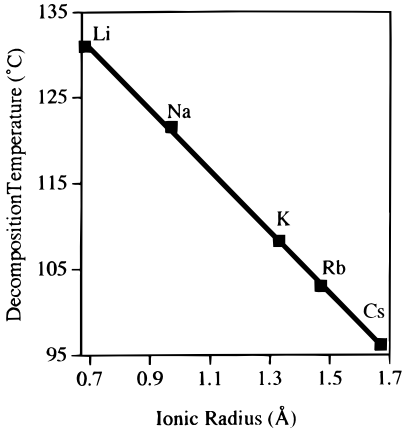

Figure 5. Decomposition temperatures versus the ionic radius of alkali metal PAO complexes.

model and lattice enthalpies predict that the decomposition reactions of metal salts of a large anion become less exothermic with increasing ionic radius of the metal.[18] Typically, a failure of the ionic model is attributed to effects of covalent bonding. In the case of the PAO salts the ring strain in the five-membered metallocycles may account for the observed trend in decomposition points. Since the chelated ligand has a small bite angle, the ring strain should increase with increasing ionic radii of the cations and thus lead to destabilization of the complexes in accord with the observed experimental data. However, it should be noted that the XRD patterns indicate that the salts are not isomorphous so that the decomposition temperatures may also be affected by differences in the crystalline lattices.

Intercalation Behavior of Sodium PAO Salts. On the basis of its layered structure, it might be expected that Na(PAO)·H_2O would be capable of forming intercalates with a variety of molecular species. Therefore, both the hydrated and dehydrated forms were stirred in dry pentane containing either pyridine or

(17) Mason, J. Nitrogen. In *Multinuclear NMR;* Mason, J., Ed.; Plenum Press: New York, 1987; p 350.

(18) Shriver, D. F.; Atkins, P. W.; Langford, C. H. *Inorganic Chemistry*; W. H. Freeman & Co.: New York, 1990; pp 123−133.

THF. However, XRD analysis indicated no change in the lattice parameters of the crystalline solid and the proton NMR spectra of a solution of the thus-treated crystals in D_2O demonstrated that none of the potential intercalating species was present. Presumably, the failure to intercalate is attributable to strong hydrogen bonds binding the layers together in the hydrate and similar strong interlayer interactions in the dehydrated compound.

Acknowledgment. We thank the Louisiana Board of Regents for support through the Louisiana Educational Quality Support Fund Contract No. LEQSF(1993-96)-RD-A-26. We also express gratitude to the National Science Foundation, who provided funds for the purchase of the solid state NMR spectrometer used in this investigation.

Supporting Information Available: Final refined parameters and tables of anisotropic thermal parameters (2 pages). X-ray crystallographic files, in CIF format, are available. Access and ordering information is given on any current masthead page.

IC9611204